Understanding and Predicting the Adsorption and Rejection of Pesticides and Metabolites by Hollow Fiber Nanofiltration Membranes

G. Dagher, G. Saab, A. Martin, G. Couturier, P. Candido, L. Moulin, Jean-Philippe Croué, B. Teychene

Understanding and Predicting the Adsorption and Rejection of Pesticides and Metabolites by Hollow Fiber Nanofiltration Membranes.

Authors: G. Dagher[1], G. Saab[1], A. Martin[2], G. Couturier[2], P. Candido[2], L. Moulin[2], JP. Croué[1], B. Teychene[1, *]

1. Institut de Chimie des Milieux et Matériaux de Poitiers (IC2MP), Université de Poitiers, CNRS, E-BiCOM, F-86073 Poitiers, France.

2. Eau de Paris, DRDQE, R&D laboratory, 33 Avenue Jean Jaurès, 94200, Ivry-Sur-Seine, France

Keywords: Pesticides and metabolites, Hollow Fiber Nanofiltration, Random forest, Micropollutants Properties.

Highlights

- The adsorption and rejection of 164 MP by HF-NF membranes is evaluated.
- The influence of 11 physicochemical properties is studied
- MP adsorption was primarily affected by log D values, followed by charge.
- MP rejection relied mainly on MP's size and charge.
- Random forest models were developed to predict MP’s adsorption and rejection.

Abstract

Layer-by-layer Hollow fiber Nanofiltration (LbL HF-NF) membranes have shown great potential in the removal of micropollutants from water. Nonetheless, further research is required as the number of tested compounds remains limited. In this study, the adsorption and rejection of 164 micropollutants by two commercial HF-NF membranes with MWCO of 400 and 800 Da, were investigated. The investigation was conducted by evaluating the influence of 11 physicochemical micropollutants' properties on the separation performances. Results showed that highly adsorbed compounds had average log D values above 3, while no or low adsorption was observed for compounds with negative log D values. Furthermore, adsorption was more frequently observed for neutral compounds compared to negatively charged ones. Micropollutants rejection results showed that steric exclusion plays the most important role in the rejection of micropollutants, and that the charge of micropollutants can also heavily influence their rejection. Likewise, negatively charged compounds were better rejected than neutral ones. Finally, the study demonstrated that adsorption and rejection of micropollutants can be predicted with good accuracy using the random forest algorithm. The prediction accuracy for adsorption was 80 % and 73 % for the 800 and 400 Da MWCO membranes, respectively. The RMSE for rejection predictions was 10.6 % and 6 % for the two membranes respectively.

1. Introduction

Climate change, droughts and pollution caused by human activities significantly impact the quality of freshwater resources. Increases in organic matter, microbial activity, algae blooms and micropollutants (MP) concentration have been widely documented in different parts of the world [1–3]. Particularly, the presence of MP in freshwater resources can be very problematic as they may have harmful effects on human health and the environment. Several technologies can be applied to remove MP from water sources like advanced oxidation processes [4], activated carbon [5], and membrane filtration [6]–[9]. Among these technologies, membrane filtration offers certain advantages like lower use of chemicals and high efficiency over a wide range of MP [6].

Nanofiltration (NF) and reverse osmosis (RO) are considered the most effective filtration methods for removing MP from water. Lipp et al. [10] studied the rejection of a selected number of compounds including pesticides, pharmaceuticals, antibiotics and perfluorinated chemicals by one RO membrane (molecular weight cut off (MWCO) of 100 Da) and three NF membranes (MWCO equal to 200, 290-360 and 200-300 Da respectively). Rejection values above 90% were found for most compounds with the four membranes. Interestingly, the rejection for NF membranes was only slightly lower than the RO membrane. Similarly, Yangali-Quintanilla et al. [11] worked on the filtration of organic contaminants and found that on average, tight NF membranes were able to effectively remove 82% of neutral contaminants and 97% of ionic contaminants. Whereas, RO membranes had an average removal rate of 85% for neutral contaminants and 99% for ionic contaminants. An analogous comparison was conducted by Jacob et al., 2012 where they examined the filtration of 30 compounds using RO and tight NF membranes and observed that 20 of the compounds exhibited similar rejections for both membranes.

As it requires less energy than RO, less post-treatment, and has a relatively good performance, the removal of MP by NF has become the focus of many studies and research. For that, the influence of MP physicochemical properties [8,13–17], organic matter [18], membrane fouling [19–21] and operating conditions [22] on MP rejection were extensively studied. In regards to the physicochemical properties specifically, several properties such as charge, molecular weight, molecular dimensions (length, width, and height), octanol-water partition coefficient (log K_{ow} or log P), and dipole moment were assessed for their effect on rejection. The charge was found to have a significant impact on the rejection as negatively charged compounds were

effectively rejected by negatively charged membranes irrespective of their other properties. Molecular weight (MW) was found to be positively correlated with rejection, particularly for neutral compounds [13,14,16]. Likewise, polarity was observed to influence rejection, as molecules with high dipole moment exhibited lower rejections overall [15,16].

Furthermore, numerous works found that the adsorption of MP on the membrane material plays a crucial role in the filtration process. If not accounted for, this adsorption can lead to an overestimation of the rejection in the filtration process [23]. The adsorption was also found to be dependent on physicochemical properties [8,14,24], membrane properties [25] and operating conditions [20,22,26,27]. In brief, the hydrophobicity of MP, typically measured by log P (or log D, the distribution coefficient), was found to be the most important property. Moreover, the impact of pH on adsorption was also observed. This impact varies among different compounds and is dependent on the specific form of each compound at different pH values.

Given the large number of factors that can affect the adsorption and rejection of MP, some researchers have turned to advanced statistical techniques and artificial intelligence-based methods to gain a more comprehensive understanding and to make predictions about the MP rejection [28–33]. Yangali-Quintanilla et al. [28] used principle component analysis and multiple linear regression to understand the impact of 21 variables on the membrane rejection and emphasized that the MP size (length, depth and width) alongside the hydrophobicity and electrostatic repulsion of the membrane are the most affecting factors. However, given that the models were created using multiple linear regression, it was only possible to get linear relations between the variables and the rejection and therefore, non-linear relations and interdependencies between variables were not taken into consideration. Jeong et al [29] were able to overcome this limitation by using a machine learning method, based on a scalable decision tree model, to predict the MP rejection. This method considered variables such as zeta potential of the membrane, MWCO, log P, hydraulic pressure, and compound concentration. They obtained a mean absolute error of 10.17% and proved that the model's predictions were primarily based on the size exclusion and electrostatic interactions between the membrane and the MP. In a similar way, a recent study by Lee and Kim [33] used random forest (RF) model for predicting NF/RO membrane rejection of emerging organic contaminants using data collected from multiples studies. They demonstrated that RF model can reliably identify important features on MP rejection with less effort than using neural network model.

The findings of these studies provide valuable insights on the removal of MP and the mechanisms behind it. However, these studies have focused on flat-sheet polyamide NF

membranes. These membranes which are housed in spiral wound modules have limited hydraulic and chemical cleaning possibilities [34]. Consequently, extensive pre-treatment, like ultrafiltration (UF) or sand filtration, is necessary to mitigate fouling on the spacers and membrane surfaces. This pre-treatment incurs additional operational costs, making it desirable to explore alternatives [35]. Recent developments in membrane fabrication techniques have allowed the production of hollow-fiber nanofiltration (HF-NF) membranes through multiple methods, with the most promising one being the coating of HF-UF membranes by polyelectrolyte multilayers (PEMs) through a layer-by-layer (LbL) coating technique [36,37]. These membranes, with their HF structure, offer a larger compacity and better cleaning capabilities than flat sheet ones, as well as high permeabilities and good selectivity. However, it is not straightforward to extrapolate results from previous research on polyamide NF membranes to HF-NF membranes. This is because they are constructed using different materials and operate at lower pressures. Moreover, the absence of a spacer in HF-NF membranes eliminates spacer-related fouling but leads to higher concentration polarization [38].

Recent studies have tested the efficiency of such membranes for MP rejection and showed promising results [39–42]. De Grooth et al. [41] synthetized NF membranes based on Polycation/Polyzwitterion/Polyanion multilayers and obtained high rejections from 50% to 99% for charged compounds with varying performance for different compounds and membranes. Ilyas et al. [42] also developed PEMs based HF-NF membranes with rejections ranging between 60% and 80% even for neutral compounds. However, these two studies used high concentrations of MP in the range of mg/L which is considered as an unrealistic condition. For that, Abtahi et al. [39] evaluated the performance of the same membranes under more realistic conditions (concentrations in the µg/L range) and achieved similar rejections (44%-77%) for the four compounds studied. Moreover, they confirmed that the hydrophobicity of these four compounds is correlated to their adsorption on the membrane surface, and that the rejection is also correlated to their molecular size.

In this regard, the number of studies on this type of membrane is still relatively scarce, especially compared to polyamide flat sheet membranes. Additionally, the number of tested MP is limited. Therefore, further research is necessary to improve the understanding of the adsorption and rejection of MP by these HF-NF membranes. As a result, this study aims to investigate the behaviour of MP on HF-NF membranes. To achieve this, the adsorption and rejection of 164 MP on commercial lab-scale modules (500 cm^2) were investigated. Notably,

the influence of MP physicochemical properties on their adsorption and rejection is highlighted and discussed. Finally, this study is concluded by an analysis based on random forest in which the adsorption and rejection of MP are predicted while highlighting the more important features.

2. Materials and methods

2.1. Nanofiltration membranes

Two commercial HF-NF lab-scale membrane modules (500 cm^2) denoted dNF40 and dNF80 were purchased from NX Filtration (Netherlands) and used in this study. According to the manufacturers, membranes of both modules are made from modified polyethersulfone (PES) and are negatively charged at pH=7. The modification of PES is performed through the LbL coating technique. Commercial modules operate in an inside-out crossflow filtration mode. They consist of 120 membrane fibers with an inside diameter of 0.7 mm and have an average surface area of 500 cm^2 (length = 30 cm). The dNF40 has a MWCO of 400 Da, a minimum $MgSO_4$ rejection of 91% and a measured permeability of 7.9 ± 0.1 $L.m^{-2}.h^{-1}.bar^{-1}$ (LMHB) at 20°C. The dNF80 has a MWCO of 800 Da, a minimum $MgSO_4$ rejection of 76% and a measured permeability of 11.6 ± 0.1 LMHB at 20°C.

2.2. Raw water

The experiments were carried out by adding the MP to a groundwater consisting of a mix of karst water from several permanent springs (Provins, France). The groundwater had a total organic carbon (TOC) content of 0.46 ± 0.06 mgC/L, UV_{254nm} absorbance equal to 0.003 ± 0.001 cm^{-1}, a turbidity of 0.1 ± 0.02 NTU, a conductivity of 584 ± 87 µS/cm, and a pH equal to 8.00 ± 0.05.

2.3. Micropollutants properties and spiking solution

A mixture of 164 MP which including 144 pesticides and other plant protection products (PPP) and 20 metabolite (M) was used in this study. The MP mixture was dissolved in a methanol solution due to water solubility limitations and was diluted in the groundwater (by a factor of 1000) to obtain MP concentrations around 1 µg/L per compound. Among these compounds, some of them were specifically chosen as metabolites of atrazine and dimethachlor, metazachlor, bentazone which are the most abundant compounds in France [43]. Information regarding the compounds present in this mixture along with their physicochemical properties are given in the supplementary data (Excel sheet).

As discussed above, the rejection and adsorption of MP by membranes are mostly influenced by size exclusion, hydrophobicity and electrostatic interactions. For that, the molar mass and molar volume were used to represent the size of these molecules. The molecular dimensions as well as the minimum projected area (MPA) were used to further understand the shape of each molecule. The three dimensions were denoted as L_1, L_2, and L_3, with L_1 being the longest side of the molecule's bounding box, L_3 being the shortest, and L_2 being the side with the median length. The octanol-water partition coefficient (log K_{ow} or log P) and the corresponding dissociation coefficient (log D) are used as a measure of hydrophobicity. The polar surface area (PSA) is used as a descriptor that quantifies molecular polarity. It represents the ability of a molecule to form hydrogen bonds with other molecules and therefore is relevant in the context of contaminants and their interactions with organic matter and membrane surfaces [44]. The polarizability was used as it may correlate with contaminants rejection and adsorption for the same reasons as the PSA. Finally, the charge at pH=8 was calculated to reflect the electrostatic interactions taking place at the membrane surface. The monoisotopic mass, the molar volume, log P, log D, the polar surface area and the polarizability were based on the calculation of ACD/Labs. pKa values as well as the charge and the minimum projected area were determined using Chemicalize by Chemaxon. The molecular dimensions were calculated using jmol software. It's worth noting that the charge of the compounds was chosen as the determining factor, rather than pKa, as opposed to previous studies. This is because large organic compounds can have multiple pKa values, making it impossible to infer the charge from just one of these values.

2.4. Filtration protocol

For all tests, cross-flow filtration with a transmembrane pressure (TMP) equal to 5 bars and a cross flow velocity of 0.3 m/s was performed using the Mexplorer^{TM} test unit (NX Filtration, Netherlands). The protocol was divided into two steps: (i) The first step was performed to study the adsorption of contaminants on the membrane surface and remove its effects before studying the rejection. In this part, the filtration was conducted while recycling the permeate within the feed tank for 48 hours. During this step, 10 mL samples of the feed and the permeate were taken at multiple occasions (t=0h, 4h, 8h, 24h, 32h and 48h) and analysed to determine the concentrations of every contaminant. Additionally, 100 mL samples of both the feed and permeate were collected at t=0h and t=48h for various measurements, including TOC, UV_{254nm} absorbance, turbidity, and pH. (ii) The second step focused on studying the rejection of MP at different recovery values. In this step, which starts at the end of the 48 hours, the permeate is

no longer recycled into the feed solution. The TMP remained at 5 bars and permeate samples were taken at recoveries of 25%, 50% and 75%. They are expressed in terms of the volume reduction factor (VRF) equal to the initial volume divided by the volume of the concentrate. The repeatability and stability of the filtration system were evaluated prior to these filtration tests on a smaller number of MP. The results indicated an average error notably smaller than the analytical error detailed in section 2.5, rendering it insignificant for consideration.

2.5. Micropollutants analysis

MP were analysed by direct injection of water samples with UHPLC-MS/MS by the laboratory of Eau de Paris accredited by the COFRAC (French Body of Accreditation). Ultra-high-performance liquid chromatography (UHPLC) was performed on a Shimadzu series Nexera X40 UHPLC system. Analytes were separated on an C18 BEH (1.7 µm 2.1×100 mm) column (Waters). Chromatographic separation of analytes was carried out with methanol and ultrapure water, both with formic acid 0.05% / ammonium acetate 5mM, in an analytical gradient from 2% to 99% methanol lasting 14 min at 0.6 mL/min. The UHPLC system was coupled to a triple-quadrupole mass spectrometer (MS/MS) Shimadzu MS 8060 with electrospray ionization (ESI) set to positive or negative mode at 350°C depending on the compound. Identification and quantification were achieved by multi reaction monitoring with 18 deuterated compounds used as injection internal standard. Analytical uncertainties are expressed as a confidence interval (α=0.05, k=2) with a mean value of 50% for the concentration between the limit of quantification (LOQ) and 5×LOQ, 30% between 5×LOQ and 50×LOQ and 20% for values above 50×LOQ.

2.6. Decision trees and random forests

A decision tree is a type of machine learning algorithm that is used for regression and classification tasks. The goal of decision trees is to learn the relationships between features and the target variable and use this information to make predictions. When applying decision trees to the filtration of MP, the features will consist of the MP physicochemical properties while the target variables are the adsorption and rejection values. Random forests are an ensemble machine learning algorithm that operates by aggregating the results of many decision trees. The concept behind random forests is to train numerous decision trees on random data subsets and then average their predictions, which results in more accurate predictions. The creation of random forests was done using RStudio and the R programming language using the “Caret” [45] and “randomForest” [46] packages. More information about decision trees and random forests and how to implement them in R can be found in James et al. [47].

3. Results and discussion

3.1. Distribution and correlation of physicochemical properties

Before studying the adsorption and rejection of the 164 MP, an assessment of the distribution of each property and the correlations between different properties was conducted to gain a better understanding of the data. The findings of both the distribution and correlations are depicted in figures 1S and 2S. To summarize, the monoisotopic mass ranged from 145 to 507 Da, while the molar volume varied from 81 to 339 cm^3/mol. The log P values ranged from -1.38 to 8.19, and the log D values ranged from -3.34 to 5.28. Additionally, the polar surface area ranged from 30 to 209 $Å^2$, while the polarizability varied from 12.6 to 45.2 $x10^{-24}$ cm^3. Among the MP assessed, 31 were negatively charged, 131 were neutral, and 2 were positively charged (at pH=8). As shown in the two figures, several correlations were observed, with the most significant ones being between the monoisotopic mass, molar volume and polarizability, and as expected between log P and log D. Good correlations were also found between the minimum projected area (MPA) and the monoisotopic mass as well as the molecular dimensions. Finally, weaker correlations were found between the monoisotopic mass and the molecular dimensions.

3.2. Adsorption of micropollutants and influence of physicochemical properties

As mentioned in section 2.4, in order to evaluate the adsorption of MP, the filtration was conducted for 48 hours while recycling the permeate and monitoring concentrations in both the feed and the permeate. By observing the variation in these concentrations, it becomes possible to understand the adsorption of MP and identify different behaviours among the tested molecules. Figure 1 illustrates this with three representative molecules, each representing a different behaviour. They are used as an example as all other compounds exhibited similar behaviour to one of these three. The first molecule, Atrazine, displayed a significant decrease in feed concentration (figure 1(a)) dropping from 0.975 µg/L to 0.04 µg/L and had very low concentration in the permeate as shown in figure 1(b). These variations in concentration suggest that Atrazine has been fully adsorbed onto the membrane surface. The second molecule, Metazachlor, exhibited a decrease in feed concentration from 0.92 µg/L to 0.49 µg/L while having an average rejection of around 75%. This decrease in concentration suggests that a fraction of Metazachlor was adsorbed on the membrane surface while the other portion remained in the feed solution. Notably, most of the decrease in concentration occurred within the first 24 hours, reaching 0.52 µg/L. This indicates that adsorption primarily occurs during

the initial 24 hours, and a steady state is approached between 24 and 48 hours. Finally, the third molecule, Dimethachlor CGA, experienced an increase in its concentration in the feed from 1.15 µg/L to 1.33 µg/L, accompanied by an average rejection of 76%. Considering the decreasing feed volume due to sample taking (260 mL of permeate) and the relatively unchanged MP mass due to high rejection, an increase in feed concentrations is anticipated, particularly if adsorption does not occur. Thus, the observed increase in feed concentration leads to the conclusion that this molecule was not adsorbed onto the membrane surface. Moreover, the major increase in concentration also occurred during the first 24 hours where the concentration reached 1.29 µg/L which confirms that a steady state is approached between 24 and 48 hours. It should be noted that Dimethachlor CGA, along with numerous other compounds, displayed initial concentrations exceeding 1 µg/L. This is attributed to the fact that the raw water used already contained trace amounts of certain compounds.

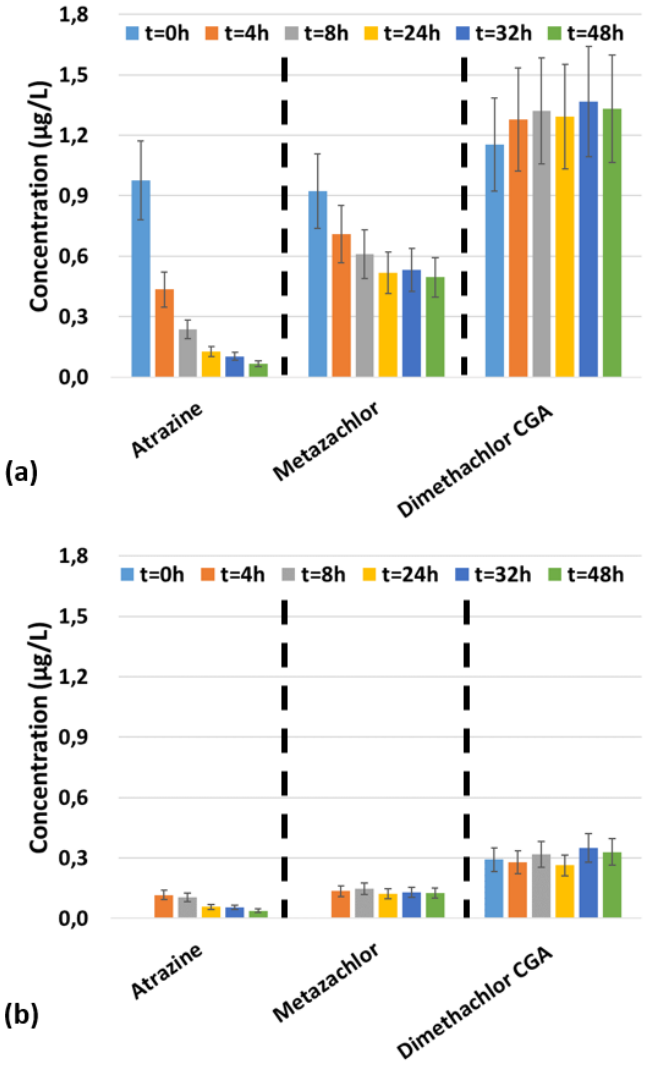

Figure 1: Variation of compounds concentration during the saturation phase in (a) the feed and (b) the permeate for filtration tests performed on the dNF80 module (Error bars corresponding to 20% confidence intervals).

Using the same approach as for these three molecules, all 164 MP compounds were classified into three adsorption categories. The first category contains compounds that showed no or low adsorption, the second category contains compounds that showed partial adsorption and the third category contains compounds that showed high or complete adsorption. More precisely, compounds that exhibited a reduction in concentration greater than 75% over the course of 48 hours were categorized as highly or completely adsorbed. Compounds that demonstrated a constant or increased concentration were assigned to the no/low adsorption class, while all other compounds were classified as partially adsorbed. The classification results are shown in the supplementary data (Excel Sheet) and summarized in table 1, which shows the number of compounds in each category. Two important points should be highlighted. First, for both membranes, the adsorption of a few compounds could not be evaluated as their initial concentrations in the feed were very low, leading to their classification as unknown (N=7 and N=5 for dNF80 and dNF40, respectively). This low concentration might be attributed to matrix effects, which can occur when numerous compounds are analysed using LC-MS, resulting in a loss or increase in response [48]. Secondly, a mass balance calculation was performed, but due to the low pollutant concentration used, the resulting values fell within the error margins. Consequently, a qualitative approach to adsorption analysis was favoured.

Table 1: Number of compounds per adsorption category

Adsorption class	**dNF80**	**dNF40**
No/Low adsorption	16 (including 7 metabolites)	32 (including 10 metabolites)
Partial adsorption	39 (including 5 metabolites)	59 (including 6 metabolites)
High/Complete adsorption	102 (including 7 metabolites)	68 (including 4 metabolites)

Upon comparing the adsorption of MP on the two membranes, it becomes evident that a significant proportion of compounds tend to adsorb more on the dNF80 membrane as compared to the dNF40 membrane. This observation can potentially be explained by the fact that, in the case of LbL coated membranes, MP adsorption is believed to occur mainly on the polymeric PES support membrane rather than on the coated layers, which is attributed to the higher hydrophobicity of PES compared to the PEMs [39, 49]. This could account for the difference in adsorption between the two membranes. In fact, as it will be discussed later, the rejection of

MP is higher for the dNF40 membrane, which might lead to fewer molecules reaching the PES support, resulting in less adsorption.

Concerning the influence of physicochemical properties, figures 2 and 3S plot the distribution of MP's physicochemical properties based on each class. The monoisotopic mass (Figures 2(a) and 2(b)) and molar volume (Figures 3S (a) and (b)) appear weakly related to adsorption as the three categories of compounds show similar distributions. However, log P (Figures 3S (c) and (d)) and log D (Figures 2(c) and (d)) exhibit significant differences between each category, indicating a strong relationship with adsorption. No adsorption was observed for compounds having negative log D values for both membranes, partial adsorption was seen for log D values around 1 for the dNF80 and around 2 for the dNF40 and high adsorption was seen for both membranes when log D values over 3. These observations are in agreement with numerous published works [14,23,25,39,49,50].

Figures 2(e) and (f) demonstrate that adsorption is related to the polar surface area, with highly adsorbed compounds having a lower polar surface area than non-adsorbed compounds for both membranes. For the dNF80 membrane, the highly adsorbed compounds had a median value equals to 56.5 $Å^2$ while the non-adsorbed compounds had a median value of 86.5 $Å^2$. For the dNF40 membranes, these values were 52.5 $Å^2$ and 92 $Å^2$ respectively. The relationship between polar surface area and adsorption is likely due to hydrophilicity. In fact, figure 1S shows that compounds with a log D value above 1 and that are partially or highly adsorbed have lower polar surface areas compared to compounds with log D values lower than 1. The polarizability (Figures 3S (e) and (f)) has a small effect on adsorption, with highly adsorbed compounds showing slightly higher values than non-adsorbed compounds for both membranes, but the difference is relatively insignificant. The charge (Figures 2(g) and (h)) also appears to have an effect on adsorption, with negatively charged compounds exhibiting low adsorption, whereas neutral compounds display partial and high adsorption, which can be attributed to the repulsion of negatively charged compounds by the membrane.

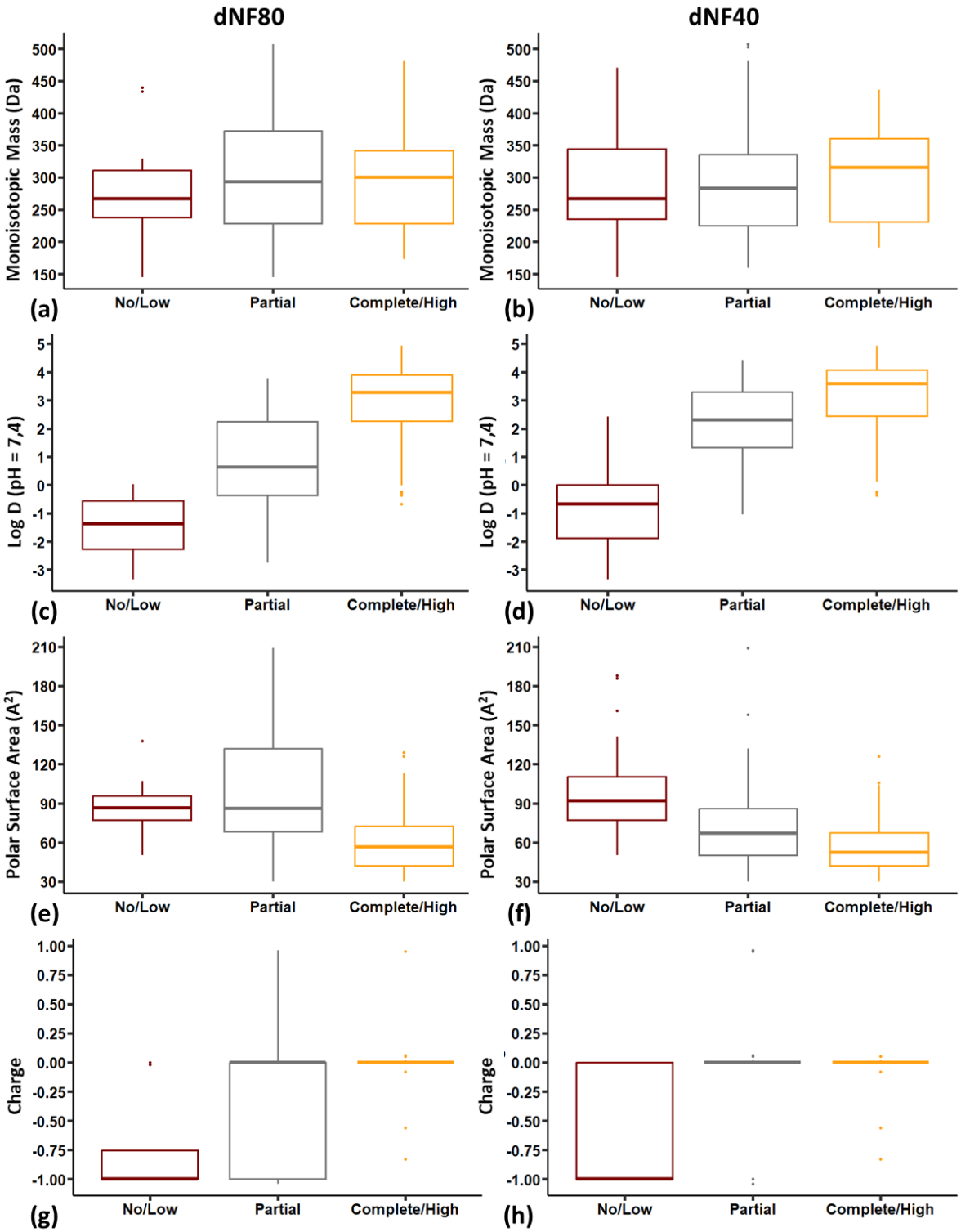

Figure 2: Boxplots showing the distribution of (a)-(b) monoisotopic mass, (c)-(d) log D, (e)-(f) polar surface area and (g)-(h) charge of MP in each adsorption category for dNF80 and dNF40 membranes

3.3. Influence of membrane MWCO, concentration and physicochemical properties on micropollutants rejection

In this part of the experiment, the rejection of MP was calculated for both membranes for a VRF of 1 and 4 (data shown in the excel sheet in supplementary data). For VRF=1, rejection was determined based on the feed and permeate concentrations measured at t=48h, while for VRF=4, the concentrations at the end of the experiment (recovery = 75%) were utilized for calculation. The calculations were made only for those compounds that were not fully adsorbed onto the membrane after 48 hours of saturation. For that, the rejection of 66 compounds for the dNF80 membrane and 101 compounds for the dNF40 membrane was determined.

Comparison of the rejection rates of the 66 common compounds demonstrates the significant impact of membrane MWCO on MP removal. The dNF40 membrane shows higher rejection values, indicating the importance of size exclusion. Ioxynil, in particular, exhibited a significant difference in rejection, with a rate of 15.3% for the dNF80 membrane compared to 85.3% for the dNF40 membrane. However, some compounds such as Clethodim, Metolachlor ESA, and Metolachlor OXA, which were highly rejected by the dNF80 membrane (>95%), showed either no change or only a small change in rejection when compared to the dNF40 membrane.

The impact of VRF on rejection was not very clear for both membranes. Most MP showed an increase in rejection at VRF = 4 (Excel Sheet), however, despite the improvement in rejection, the concentrations of MP in the permeate at VRF = 4 (75% recovery) were consistently higher than the initial concentrations (VRF = 1). This suggests that while rejections are improving, the water quality is slightly worsening.

The correlation between rejection and various physicochemical properties was also examined as shown in Figures 3, 4 and 4S. To begin, the influence of the charge was assessed for both membranes (shown in figure 3). In the case of the dNF80 membrane (figure 3(a)), it is evident that negatively charged compounds tend to be well rejected, with most compounds exhibiting a rejection rate of over 80%, while the rejection rate of neutral compounds varied from 0.47% to 99% depending on the compound. For the dNF40 membrane (figure 3(b)), the rejection rate was relatively high for all compounds regardless of their charge, with only a few exceptions for certain neutral compounds. The number of positively charged compounds is too low to draw any conclusions, so they will be disregarded for the remainder of the study.

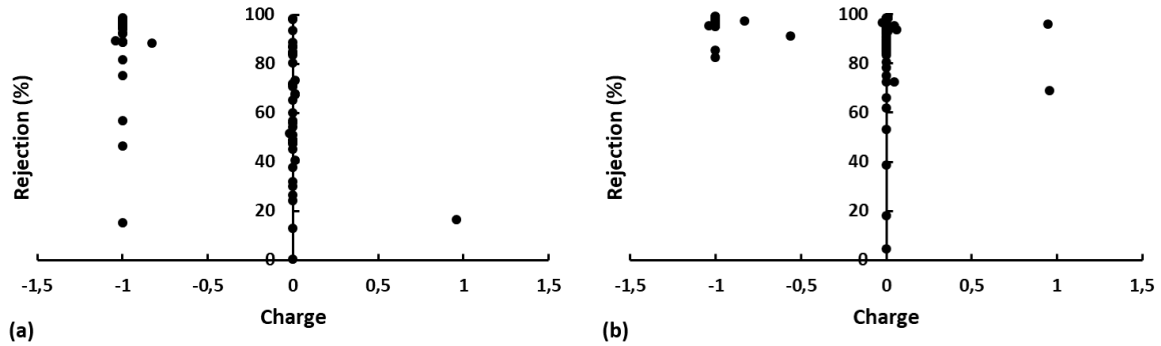

Figure 3: Rejection of MP (VRF=1) function of the charge for the (a) dNF80 membrane and (b) dNF40 membrane

When comparing the rejection in terms of the monoisotopic mass (figures 4(a) and 4(b)), results show that negatively charged compounds are effectively rejected by the dNF80 membrane at a monoisotopic mass of 250 Da, while the dNF40 membrane effectively rejects all negatively charged compounds with a mass as low as 210 Da. One molecule, Ioxynil, stands out as it does not follow the trend of negatively charged compounds on the dNF80 membrane and has low rejection. However, this could be due to the fact that Ioxynil is a small 2-dimensional molecule (Molar volume = 136.7 cm^3/mol, L_3 = 0 Å) with a large monoisotopic mass resulting from the presence of two iodine atoms. Neutral compounds are better rejected by the dNF80 membrane as their monoisotopic mass increases from 145 Da to 380 Da, with rejection rates increasing from less than 1% to over 90%. The dNF40 membrane effectively rejects neutral compounds starting at a mass of 200 Da, which is consistent with previous research [51]. Moreover, there is a notable threshold between 150 and 200 Da, where rejection rates increase rapidly from approximately 4% to over 80%. Similar conclusions could be drawn regarding the effect of the molar volume (figure 4S (a) and (b)), which is well-correlated with monoisotopic mass (figure 1S).

Figures 4 (c) and (d) indicate that the relationship between membrane rejection and log D is not well-established (as well as Log P given the correlation between log P and log D, as shown in figure 4S (c) and (d)). Negatively charged compounds, which have typically a negative log D, are effectively rejected by both membranes. For neutral compounds, hydrophobic compounds with higher log D values seem to be better rejected than hydrophilic ones, but it is uncertain whether log D is the only factor influencing the rejection, or if other properties also play a role. For example, Spirotetramat has a log D of 3.79 and a rejection rate of 93.5% (dNF80, VRF=1), but exhibits also a monoisotopic mass of 373.2 Da much higher than the membrane MWCO. Additionally, many compounds with log D > 2 for dNF80 and log D > 3 for dNF40 were

completely adsorbed on the membrane surface, so their rejection rates could not be calculated. Therefore, the influence of log D and hydrophobicity cannot be confirmed, despite the presence of some trends.

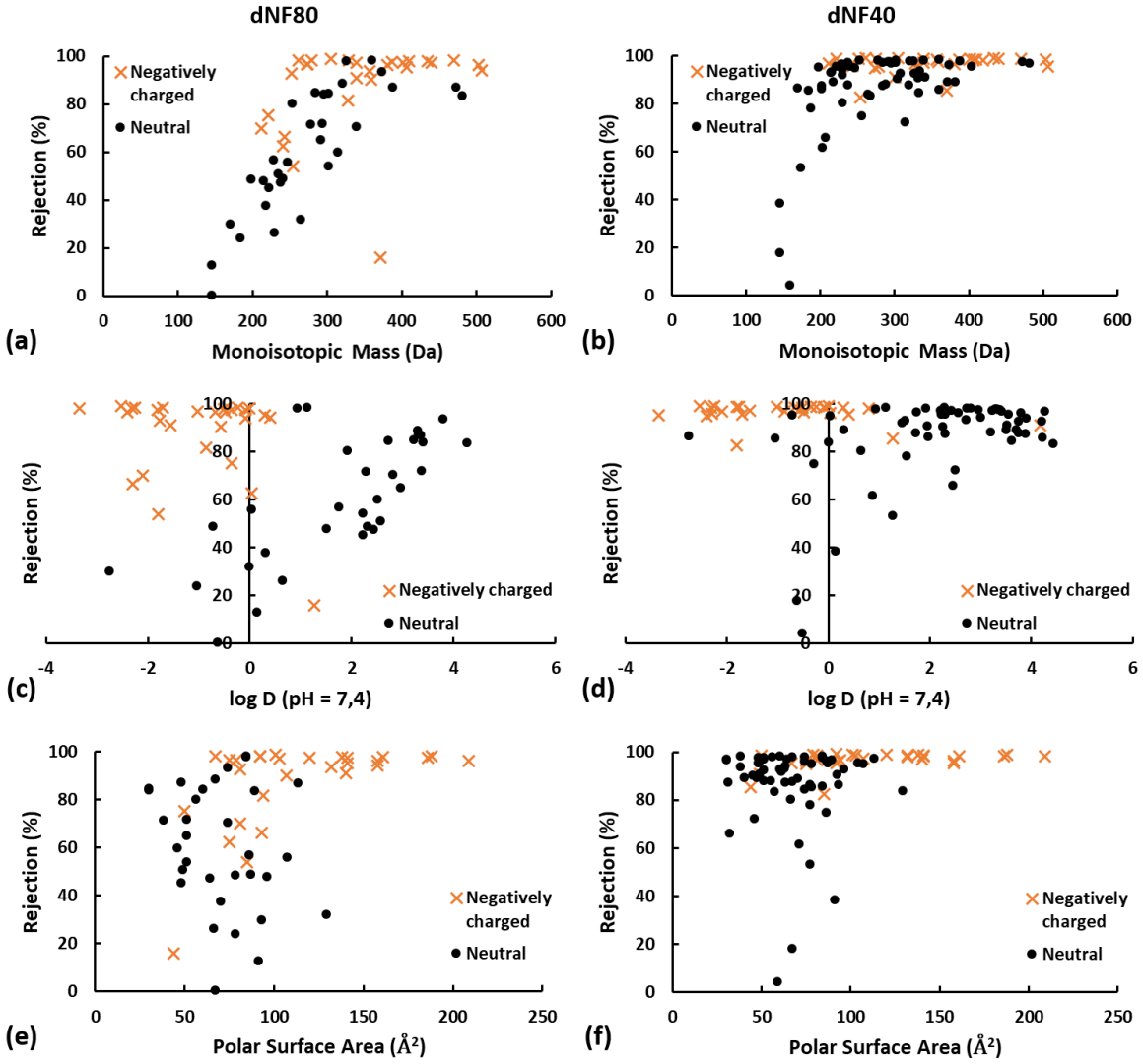

Figure 4: Rejection of MP (VRF=1) function of (a)-(b) the monoisotopic mass, (c)-(d) log D and (e)-(f) the polar surface for the dNF80 and dNF40 membranes

Concerning the polar surface area, the rejection of negatively charged compounds by the dNF80 membrane (figure 4(e)) was higher for compounds having a polar surface area higher than 100 $Å^2$. Apart from that, no effect of polar surface area on rejection was observed for the neutral compounds on the same membrane. Additionally, like mentioned before, the rejection of most compounds by the dNF40 membrane (figure 4(f)) was high which made it difficult to notice any trend in case it existed. For the polarizability (figure 4S (e) and (f)), given that it was highly correlated with the monoisotopic mass and the molar volume as presented early on, similar variations were observed.

The relationship between rejection and molecular dimensions was also examined as displayed in figure 5S. In contrast to previous studies [31,52,53], no clear association was found between rejection and any of the dimensions. Nonetheless, on the dNF80 membrane, a moderate correlation was observed between rejection of neutral compounds and L_1 ($R^2 = 0.52$) as well as L_3 ($R^2 = 0.67$), with rejection rates increasing as L_1 and L_3 increased. Additionally, while previous research has reported a strong correlation between rejection and MPA [39, 52], present results did not reveal any correlation between MPA and rejection for the two membranes, as shown in Figure 6S (a) and (b).

In summary, the analysis of MP rejection by HF-NF membranes in relation to their physicochemical properties and membrane MWCO yielded several observations. Steric exclusion was a crucial factor in rejection, evidenced by higher rejection rates with the dNF40 membrane and the correlation between monoisotopic mass and rejection of neutral compounds by the dNF80 membrane. MP electrostatic charge also played a significant role, with negatively charged compounds being generally better rejected than neutral ones. Additionally, some properties like log D and polar surface area may affect rejection, but further investigation is needed. Finally, contrary to previous findings, only moderate and weak correlations were found between rejection and molecular dimensions and no correlation was found with MPA. In the following, a random forest model was developed to confirm these main features and investigate the rejection mechanisms of HF-NF membranes.

3.4. Application of random forest on the filtration of micropollutants

Based on the results in sections 3.2 and 3.3, it is possible to say that the adsorption and rejection of MP are the result of the interplay between various properties related to the MP and the membrane. For that, given the complexity of these subjects and the impossibility of creating straightforward guidelines for the adsorption and rejection of MP by HF-NF membranes, the use of artificial intelligence has become crucial to estimate MP's adsorption and rejection. In the following, an attempt to predict the adsorption and rejection of the 164 MP was tested. First, available data was randomly divided into training and testing data, with the former containing 80% of the total data. Then, random forests were applied on training data and used to predict the adsorption and rejection of the testing data.

Among the properties studied in this work, four properties were selected to predict the adsorption and rejection of MP. These properties are the monoisotopic mass, the charge, log D and the polar surface area. The choice was based on the correlation matrix presented in figures

1S and 2S and on the observed impact of each property. Specifically, when two properties were found to be correlated, such as the monoisotopic mass and molar volume, only one was selected. Conversely, properties that showed no or weak relation to adsorption or rejection, like molecular dimensions, were disregarded.

The classification of MP into the three adsorption categories by random forests was tested on the testing data set. A model was created for each membrane (dNF40 or dNF80) and results are presented in the form of confusion matrices in tables 2 and 3. Table 2 shows the results of the prediction of the adsorption of 30 compounds on the dNF80 membrane. In this table, 3 compounds correspond to the "No/low" adsorption category, 7 to the "Partial" adsorption category and 20 to the "Complete/High" category. Out of these compounds 24 were correctly classified (represented by the grey squares) and thus an 80% accuracy was obtained. Likewise, for the adsorption on the dNF40 membrane (table 3), 22 compounds out of 30 were correctly classified resulting in a 73% accuracy. Furthermore, when applying random forests to predict a certain response it is possible to determine the degree of importance of the variables used to make the predictions. For the adsorption of MP, log D was found to be the most important property for both membranes followed by the charge, then the polar surface area and finally the monoisotopic mass (figure 5). This corresponds well to the conclusions that were deducted in the previous paragraph (section 3.2).

Table 2: Confusion matrix comparing between the predicted and the observed adsorption behaviour on the dNF80 membrane

dNF80		**Observed**		
		No/Low	**Partial**	**Complete/High**
Predicted	**No/Low**	2	1	0
	Partial	0	4	2
	Complete/High	1	2	18

Table 3: Confusion matrix comparing between the predicted and the observed adsorption behaviour on the dNF40 membrane

dNF40		**Observed**		
		No/Low	**Partial**	**Complete/High**
Predicted	**No/Low**	4	2	0
	Partial	2	7	2
	Complete/High	0	2	11

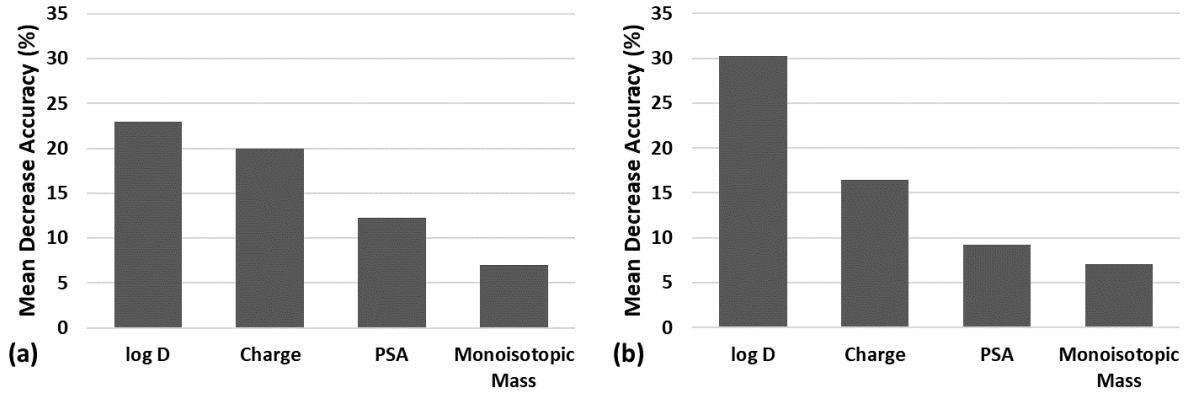

Figure 5: Feature importance for adsorption prediction on (a) the dNF80 membrane and (b) the dNF40 membrane

Regarding the rejection of MP, a comparison between the predicted and calculated values is presented in figure 6. For the dNF80 membrane (figure 6(a)), the rejection was predicted with a residual mean squared error (RMSE) of 10.6%. Similarly, for the dNF40 membrane (Figure 6(b)), an RMSE of 6% was obtained. In terms of physicochemical properties importance (figure 7), the monoisotopic mass was deemed the most significant property for rejection on both membranes followed by the charge, log D and the polar surface area respectively. It is worth mentioning that Ioxynil, despite showing an outlier rejection on the dNF80 membrane, was included in the training data for the random forest model. This decision was made because the presence or absence of Ioxynil did not have a significant impact on the results.

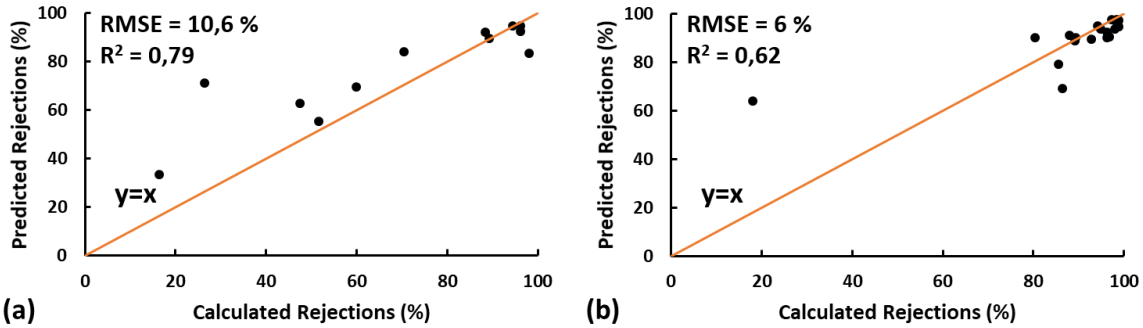

Figure 6: Comparison between the predicted and calculated rejection by (a) the dNF80 membrane and (b) the dNF40 membrane

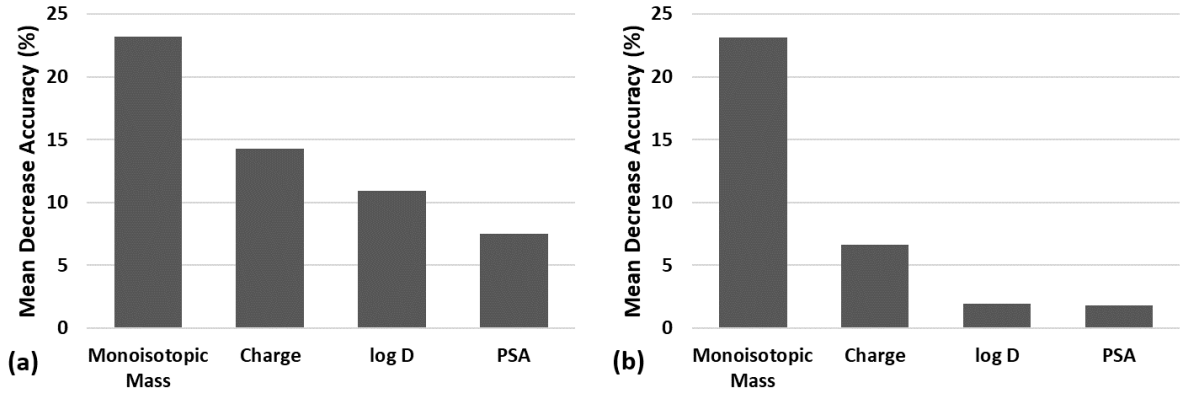

Figure 7: Feature importance for rejection prediction on the (a) dNF80 membrane and (b) dNF40 membrane

These results demonstrate that the adsorption and rejection of MP can be predicted with a relatively high degree of accuracy no matter their nature (metabolites or PPP). Nonetheless, it is essential to recognize that each model is constrained by the specific operating conditions under which the data is collected. If any parameter is altered, resulting in different rejection and adsorption outcomes, the random forest model cannot accurately predict these new values, as it was trained on different data. For instance, variations in pH can lead to changes in some log D values, affecting the hydrophobicity of the compounds and thereby altering their adsorption behaviour. The same principle applies to any other influencing factor. To achieve reliable predictions, it is crucial to either build a new model when the operating conditions change or incorporate these conditions into the model, whenever possible. Once the model had been established, it can then be used to predict the behaviour of new compounds with similar properties.

4. Conclusion

This study investigated the influence of MP physicochemical properties on their adsorption and rejection by HF LbL coated NF membranes. Two membranes with MWCOs of 400 Da and 800 Da were tested. The experimental procedure involved a two-step filtration test using a mixture of 164 compounds. The first step evaluated adsorption during a 48-hour saturation period, while the second step determined rejection at different recoveries.

Based on behaviour during the saturation period, compounds were classified into three categories, with hydrophobicity (log D) and charge being crucial for adsorption. Compounds with negative log D values showed little to no adsorption, while highly adsorbed ones had log D > 3 for both membranes. Moreover, negatively charged compounds were less adsorbed compared to neutral compounds. Regarding MP rejection, steric exclusion and electrostatic

repulsion played major roles. The 400 Da MWCO membrane had higher rejection rates for all compounds than the 800 Da MWCO membrane. Also, negatively charged compounds were better rejected, while neutral compounds showed varying rejection rates. Additionally, log D and polar surface area were observed to potentially impact rejection, although additional research is necessary. In contrast to prior research, rejection showed only moderate and weak correlations with molecular dimensions, and no correlation was observed with MPA.

Finally, the study demonstrated that artificial intelligence, specifically random forests, could predict MP adsorption and rejection with relatively good accuracy. The adsorption prediction accuracy was 80% and 73%, and the rejection prediction RMSE values were 10.6% and 6% for the dNF80 and dNF40 membranes, respectively.

To further advance the study, future research should aim to investigate the adsorption and rejection behaviour of the membranes on larger scale modules. The saturation period should be extended with continuous addition of MP to the feed to better understand the behaviour of adsorbed compounds during and after saturation. It is possible that some rejection results might be overestimated if the 48-hour saturation period is not sufficient, hence warranting a more extended saturation period. Additionally, it is interesting to investigate the individual behaviour of MP and compare it to their behaviour within mixtures. While testing each of the 164 compounds individually might not be practical, it can be performed on selected molecules. Besides that, the inclusion of more positively charged compounds can aid in evaluating their behaviour during the filtration process. And last, it is recommended to explore the effects of achieving higher recovery values and the influence of operating conditions like the transmembrane pressure and crossflow velocity.

Acknowledgments:

The authors acknowledge financial support from the European Union (ERDF) and Région Nouvelle Aquitaine. This work pertains to the French government program "Investissements d'Avenir" (EUR INTREE, reference ANR-18-EURE-0010). The authors would also like to thank NX filtration for providing the membranes.

Author Contribution

G. Dagher: Methodology, Analysis, Writing. **G. Saab:** Experimentation. **A. Martin:** Methodology, Review and Editing. **G. Couturier and P. Candido:** UHPLC-MS/MS analysis.

L. Moulin and JP. Croué: Review and Editing. **B. Teychene:** Conceptualization, Resources, Methodology, Supervision, Review and Editing.

5. References

[1] P. Beaudeau, M. Pascal, D. Mouly, C. Galey, and O. Thomas, Health risks associated with drinking water in a context of climate change in France: a review of surveillance requirements, *J. Water Clim. Change*. 2 (2011) 230–246. doi: 10.2166/wcc.2011.010.

[2] A. Mishra, A. Alnahit, and B. Campbell, Impact of land uses, drought, flood, wildfire, and cascading events on water quality and microbial communities: A review and analysis, *J. Hydrol.* 596 (2021) doi: 10.1016/j.jhydrol.2020.125707.

[3] L. M. Mosley, Drought impacts on the water quality of freshwater systems; review and integration, *Earth-Sci. Rev.* 140 (2015) 203–214. doi: 10.1016/j.earscirev.2014.11.010.

[4] R. Yin and C. Shang, Removal of micropollutants in drinking water using UV-LED/chlorine advanced oxidation process followed by activated carbon adsorption, *Water Res.* 185 (2020). doi: 10.1016/j.watres.2020.116297.

[5] M. Boehler, B. Zwickenpflug, J. Hollender, T. Ternes, A. Joss, and H. Siegrist, Removal of micropollutants in municipal wastewater treatment plants by powder-activated carbon, *Water Sci. Technol.* 66 (2012). doi: 10.2166/wst.2012.353.

[6] N. K. Khanzada *et al.*, Removal of organic micropollutants using advanced membrane-based water and wastewater treatment: A review, *J. Membr. Sci.* 598 (2020). doi: 10.1016/j.memsci.2019.117672.

[7] Y. S. Khoo *et al.*, Removal of emerging organic micropollutants via modified-reverse osmosis/nanofiltration membranes: A review, *Chemosphere*. 305 (2022). doi: 10.1016/j.chemosphere.2022.135151.

[8] P. Xu *et al.*, Rejection of Emerging Organic Micropollutants in Nanofiltration–Reverse Osmosis Membrane Applications, *Water Environ. Res.* 77 (2005) doi: 10.2175/106143005X41609.

[9] S. Kim *et al.*, Removal of contaminants of emerging concern by membranes in water and wastewater: A review, *Chem. Eng. J.* 335 (2018). doi: 10.1016/j.cej.2017.11.044.

[10] P. Lipp, F. Sacher, and G. Baldauf, Removal of organic micro-pollutants during drinking water treatment by nanofiltration and reverse osmosis, *Desalination Water Treat.* 13 (2010). doi: 10.5004/dwt.2010.1063.

[11] V. Yangali-Quintanilla, S. K. Maeng, T. Fujioka, M. Kennedy, and G. Amy, Proposing nanofiltration as acceptable barrier for organic contaminants in water reuse, *J. Membr. Sci.* 362 (2010). doi: 10.1016/j.memsci.2010.06.058.

[12] M. Jacob, C. Li, C. Guigui, C. Cabassud, G. Lavison, and L. Moulin, Performance of NF/RO process for indirect potable reuse: interactions between micropollutants, micro-organisms and real MBR permeate, *Desalination Water Treat.* 46 (2012) doi: 10.1080/19443994.2012.677507.

[13] P. Berg, G. Hagmeyer, and R. Gimbel, Removal of pesticides and other micropollutants by nanofiltration, *Desalination*. 113 (1997) doi: 10.1016/S0011-9164(97)00130-6.

[14] K. Kimura, G. Amy, J. E. Drewes, T. Heberer, T.-U. Kim, and Y. Watanabe, Rejection of organic micropollutants (disinfection by-products, endocrine disrupting compounds, and pharmaceutically active compounds) by NF/RO membranes, *J. Membr. Sci.* 227 (2003). doi: 10.1016/j.memsci.2003.09.005.

[15] B. Van der Bruggen, J. Schaep, W. Maes, D. Wilms, and C. Vandecasteele, Nanofiltration as a treatment method for the removal of pesticides from ground waters, *Desalination*. 117 (1998). doi: 10.1016/S0011-9164(98)00081-2.

[16] B. Van der Bruggen, J. Schaep, D. Wilms, and C. Vandecasteele, Influence of molecular size, polarity and charge on the retention of organic molecules by nanofiltration, *J. Membr. Sci.* 156 (1999). doi: 10.1016/S0376-7388(98)00326-3.

[17] A. Verliefde, E. Cornelissen, G. Amy, B. Van der Bruggen, and H. van Dijk, Priority organic micropollutants in water sources in Flanders and the Netherlands and assessment of removal possibilities with nanofiltration, *Environ. Pollut.* 146 (2007). doi: 10.1016/j.envpol.2006.01.051.

[18] A. De Munari, A. J. C. Semiao, and B. Antizar-Ladislao, Retention of pesticide Endosulfan by nanofiltration: Influence of organic matter–pesticide complexation and solute–membrane interactions, *Water Res.* 47 (2013). doi: 10.1016/j.watres.2013.03.055.

[19] K. O. Agenson and T. Urase, Change in membrane performance due to organic fouling in nanofiltration (NF)/reverse osmosis (RO) applications, *Sep. Purif. Technol.* 55 (2007) doi: 10.1016/j.seppur.2006.11.010.

[20] Y.-L. Lin, Effects of organic, biological and colloidal fouling on the removal of pharmaceuticals and personal care products by nanofiltration and reverse osmosis membranes, *J. Membr. Sci.* 542 (2017). doi: 10.1016/j.memsci.2017.08.023.

609 [21] L. D. Nghiem, P. J. Coleman, and C. Espendiller, Mechanisms underlying the effects of
610 membrane fouling on the nanofiltration of trace organic contaminants, *Desalination*, 250
611 (2010).doi: 10.1016/j.desal.2009.03.025.
612 [22] A. Imbrogno and A. I. Schäfer, Micropollutants breakthrough curve phenomena in
613 nanofiltration: Impact of operational parameters, *Sep. Purif. Technol.* 267 (2021). doi:
614 10.1016/j.seppur.2021.118406.
615 [23] K. Kimura, G. Amy, J. Drewes, and Y. Watanabe, Adsorption of hydrophobic compounds
616 onto NF/RO membranes: an artifact leading to overestimation of rejection, *J. Membr. Sci.*
617 221 (2003). doi: 10.1016/S0376-7388(03)00248-5.
618 [24] B. Van der Bruggen *et al.*, Assessment of a semi-quantitative method for estimation of the
619 rejection of organic compounds in aqueous solution in nanofiltration, *J. Chem. Technol.*
620 *Biotechnol.* 81 (2006). doi: 10.1002/jctb.1489.
621 [25] A. J. C. Semião and A. I. Schäfer, Removal of adsorbing estrogenic micropollutants by
622 nanofiltration membranes. Part A—Experimental evidence, *J. Membr. Sci.* 431 (2013).
623 doi: 10.1016/j.memsci.2012.11.080.
624 [26] J. L. Acero, F. J. Benitez, F. Teva, and A. I. Leal, Retention of emerging micropollutants
625 from UP water and a municipal secondary effluent by ultrafiltration and nanofiltration,
626 *Chem. Eng. J.* 163 (2010). doi: 10.1016/j.cej.2010.07.060.
627 [27] A. J. C. Semião and A. I. Schäfer, Estrogenic micropollutant adsorption dynamics onto
628 nanofiltration membranes, *J. Membr. Sci.* 381 (2011). doi:
629 10.1016/j.memsci.2011.07.031.
630 [28] V. Yangali-Quintanilla, A. Sadmani, M. McConville, M. Kennedy, and G. Amy, A QSAR
631 model for predicting rejection of emerging contaminants (pharmaceuticals, endocrine
632 disruptors) by nanofiltration membranes, *Water Res.* 44 (2010). doi:
633 10.1016/j.watres.2009.06.054.
634 [29] N. Jeong, T. Chung, and T. Tong, Predicting Micropollutant Removal by Reverse Osmosis
635 and Nanofiltration Membranes: Is Machine Learning Viable?, *Environ. Sci. Technol*. 55
636 (2021). doi: 10.1021/acs.est.1c04041.
637 [30] B. Teychene *et al.*, Investigation of polar mobile organic compounds (PMOC) removal by
638 reverse osmosis and nanofiltration: rejection mechanism modelling using decision tree,
639 *Water Supply* 20 (2020). doi: 10.2166/ws.2020.020.
640 [31] S. Sanches, C. F. Galinha, M. T. Barreto Crespo, V. J. Pereira, and J. G. Crespo,
641 Assessment of phenomena underlying the removal of micropollutants during water

treatment by nanofiltration using multivariate statistical analysis, *Sep. Purif. Technol.* 118 (2013). doi: 10.1016/j.seppur.2013.07.020.

[32] A. Shahmansouri and C. Bellona, Application of quantitative structure–property relationships (QSPRs) to predict the rejection of organic solutes by nanofiltration, *Sep. Purif. Technol.* 118 (2013). doi: 10.1016/j.seppur.2013.07.050.

[33] S. Lee and J. Kim, Prediction of Nanofiltration and Reverse-Osmosis-Membrane Rejection of Organic Compounds Using Random Forest Model, *J. Environ. Eng.* 146 (2020). doi: 10.1061/(ASCE)EE.1943-7870.0001806.

[34] A. Al-Amoudi and R. W. Lovitt, Fouling strategies and the cleaning system of NF membranes and factors affecting cleaning efficiency, *J. Membr. Sci.* 303 (2007). doi: 10.1016/j.memsci.2007.06.002.

[35] F. Vince, E. Aoustin, P. Bréant, and F. Marechal, LCA tool for the environmental evaluation of potable water production, *Desalination*. 220 (2008). doi: 10.1016/j.desal.2007.01.021.

[36] A. Toutianoush, W. Jin, H. Deligöz, and B. Tieke, Polyelectrolyte multilayer membranes for desalination of aqueous salt solutions and seawater under reverse osmosis conditions, *Appl. Surf. Sci.* 246 (2005) doi: 10.1016/j.apsusc.2004.11.068.

[37] N. Joseph, P. Ahmadiannamini, R. Hoogenboom, and I. F. J. Vankelecom, Layer-by-layer preparation of polyelectrolyte multilayer membranes for separation, *Polym. Chem.* 5 (2014). doi: 10.1039/C3PY01262J.

[38] W. A. Jonkers, E. R. Cornelissen, and W. M. de Vos, Hollow fiber nanofiltration: From lab-scale research to full-scale applications, *J. Membr. Sci.* 669 (2023) doi: 10.1016/j.memsci.2022.121234.

[39] S. M. Abtahi, S. Ilyas, C. Joannis Cassan, C. Albasi, and W. M. de Vos, Micropollutants removal from secondary-treated municipal wastewater using weak polyelectrolyte multilayer based nanofiltration membranes, *J. Membr. Sci.* 548 (2018). doi: 10.1016/j.memsci.2017.10.045.

[40] S. M. Abtahi *et al.*, Micropollutant rejection of annealed polyelectrolyte multilayer based nanofiltration membranes for treatment of conventionally-treated municipal wastewater, *Sep. Purif. Technol.* 209 (2019). doi: 10.1016/j.seppur.2018.07.071.

[41] J. De Grooth, D. M. Reurink, J. Ploegmakers, W. M. de Vos, and K. Nijmeijer, Charged Micropollutant Removal With Hollow Fiber Nanofiltration Membranes Based On Polycation/Polyzwitterion/Polyanion Multilayers, *ACS Appl. Mater. Interfaces*, 6 (2014). doi: 10.1021/am504630a.

[42] S. Ilyas, S. M. Abtahi, N. Akkilic, H. D. W. Roesink, and W. M. de Vos, Weak polyelectrolyte multilayers as tunable separation layers for micro-pollutant removal by hollow fiber nanofiltration membranes, *J. Membr. Sci.*, 537 (2017). doi: 10.1016/j.memsci.2017.05.027.

[43] N. Baran, A. E. Rosenbom, R. Kozel, and D. Lapworth, Pesticides and their metabolites in European groundwater: Comparing regulations and approaches to monitoring in France, Denmark, England and Switzerland, *Sci. Total Environ.*, 842 (2022). doi: 10.1016/j.scitotenv.2022.156696.

[44] G. Caron and G. Ermondi, Molecular descriptors for polarity: the need for going beyond polar surface area, *http://dx.doi.org/10.4155/fmc-2016-0165*, (2016).

[45] K. Max, Building Predictive Models in R Using the caret Package, *J. Stat. Softw.*, 28 (2008). doi: 10.18637/jss.v028.i05.

[46] A. Liaw and M. Wiener, Classification and Regression by RandomForest, *Forest*, 23 (2001)

[47] G. James, D. Witten, T. Hastie, and R. Tibshirani, *An Introduction to Statistical Learning: with Applications in R*. New York, NY: Springer US, 2021. doi: 10.1007/978-1-0716-1418-1.

[48] W. Zhou, S. Yang, and P. G. Wang, Matrix effects and application of matrix effect factor, *Bioanalysis*, 9 (2017). doi: 10.4155/bio-2017-0214.

[49] A. R. D. Verliefde *et al.*, Influence of Solute−Membrane Affinity on Rejection of Uncharged Organic Solutes by Nanofiltration Membranes, *Environ. Sci. Technol.*, 43 (2009). doi: 10.1021/es803146r.

[50] H. Xu *et al.*, A Simple Method to Identify the Dominant Fouling Mechanisms during Membrane Filtration Based on Piecewise Multiple Linear Regression, *Membranes*, 10 (2020). doi: 10.3390/membranes10080171.

[51] S. van der Poel, Parting ways – removal of salts and organic micropollutants by direct nanofiltration: Pretreatment of surface water for the production of dune infiltration water, 2020, Accessed: Feb. 23, 2023. [Online]. Available: https://repository.tudelft.nl/islandora/object/uuid%3A6774b91c-6850-4c82-b3c0-a3110f0c40b9

[52] T. Fujioka, S. J. Khan, J. A. McDonald, and L. D. Nghiem, Nanofiltration of trace organic chemicals: A comparison between ceramic and polymeric membranes, *Sep. Purif. Technol.*, 136 (2014). doi: 10.1016/j.seppur.2014.08.039.

709 [53] Y. Kiso *et al.*, Effect of molecular shape on rejection of uncharged organic compounds by
710 nanofiltration membranes and on calculated pore radii, *J. Membr. Sci.*, 358 (2010). doi:
711 10.1016/j.memsci.2010.04.034.